Science Advances
AAAS

advances.sciencemag.org/cgi/content/full/5/1/eaav0216/DC1

Supplementary Materials for

MRGPR-mediated activation of local mast cells clears cutaneous bacterial infection and protects against reinfection

Mohammad Arifuzzaman, Yuvon R. Mobley, Hae Woong Choi, Pradeep Bist, Cristina A. Salinas, Zachary D. Brown, Swaine L. Chen, Herman F. Staats, Soman N. Abraham*

*Corresponding author. Email: soman.abraham@duke.edu

Published 2 January 2019, *Sci. Adv.* **5**, eaav0216 (2019)
DOI: 10.1126/sciadv.aav0216

This PDF file includes:

Table S1. Antibacterial and MC-activating capacities of mastoparan analog peptides.

Peptide[1]	MIC (μg/ml)[2]	Degranulation >5% by 25 μM
13L	32	Yes
6K	X	No
6A	X	No
6C	X	No
6D	X	No
6E	X	No
6F	124	No
6G	X	No
6H	X	No
6I	32	No
6M	124	No
6N	X	No
6P	X	No
6Q	X	No
6W	X	Yes

[1]The number indicates position of the single amino acid substitution and the letter represents single-letter code for the substituting amino acid.

[2]The X indicates MIC > 500 μg/ml

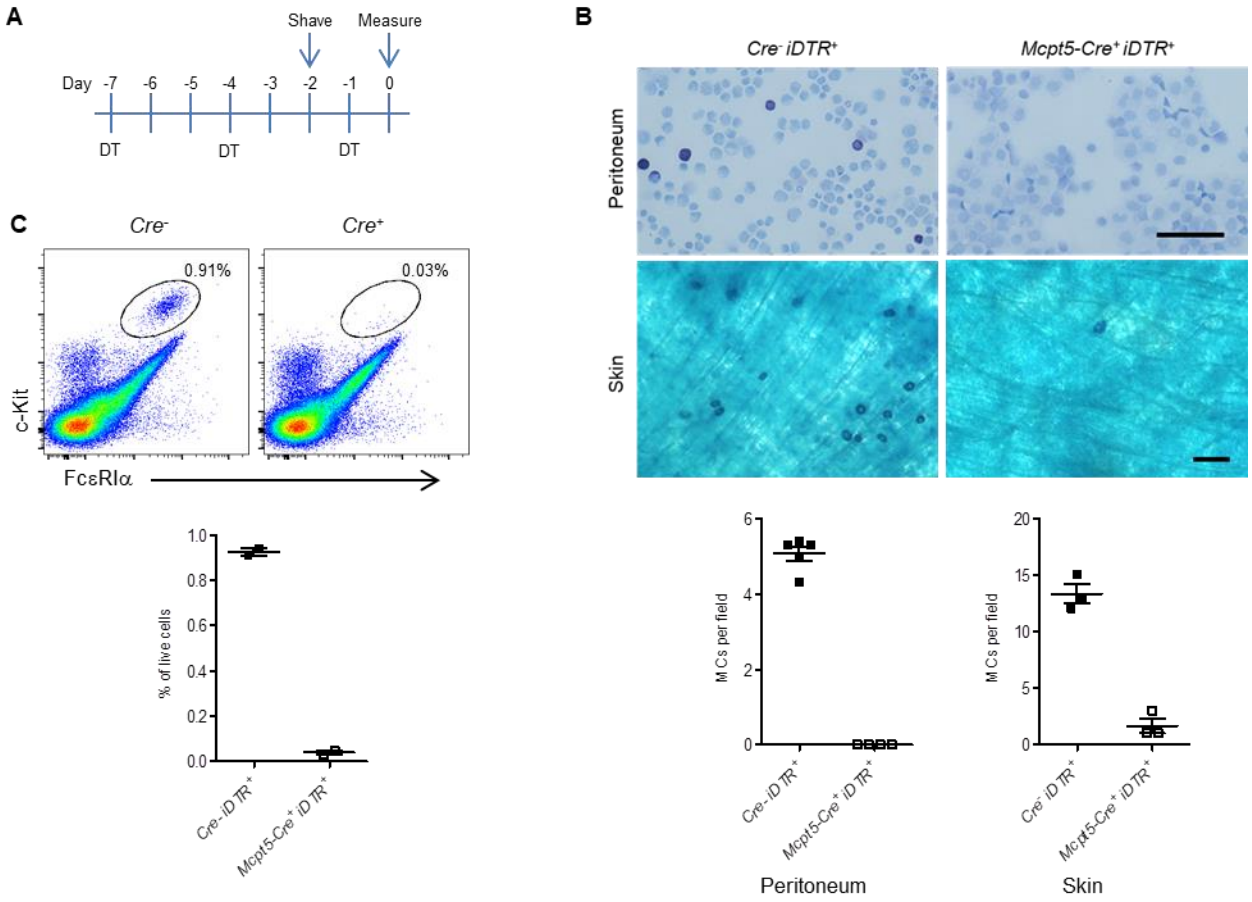

Fig. S1. Depletion of CTMCs. (**A**) Schematic plan for CTMC depletion. Depletion of CTMCs was achieved by treating *Mcpt5-Cre*$^{+}$ *iDTR*$^{+}$ mice or littermate controls (*Cre*$^{-}$ *iDTR*$^{+}$) intraperitoneally and subcutaneously with diphtheria toxin (DT) every 3rd day for seven days. (**B**) Representative images of granulated mast cells stained with toluidine blue in peritoneal lavage or dorsal skin whole mount 24 hours after 3rd dose of DT. Scale bar 10 µm. Graphs at the bottom show depletion of MCs in *Mcpt5-Cre*$^{+}$*iDTR*$^{+}$ mice compared to control (*Cre*$^{-}$ *iDTR*$^{+}$) mice. (**C**) Representative flow cytometry plots showing FcεRIα^{+} c-Kit^{+} MCs in single cell suspensions from infected *Cre*$^{-}$ and *Cre*$^{+}$ mice. Graph at the bottom shows percentage of MCs (n = 2).

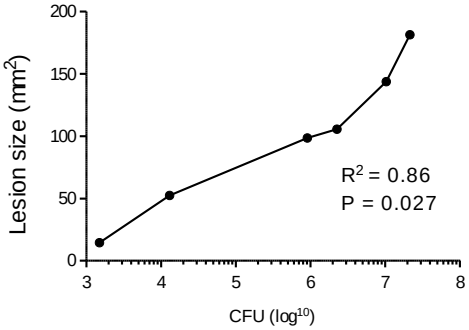

Fig. S2. Correlation between CFU and lesion size. In the dermonecrotic *S. aureus* infection model, skin samples were collected at various days post infection. R indicates the Person's correlation coefficient.

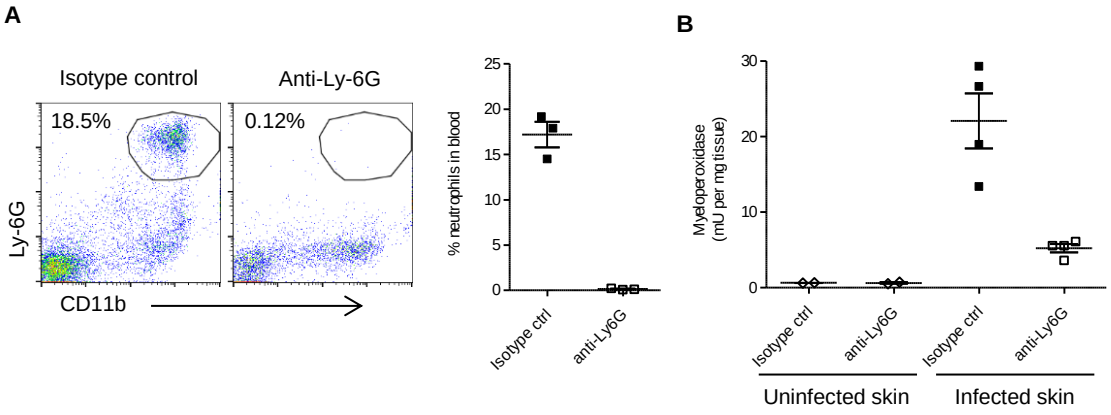

Fig. S3. Depletion of neutrophils. (**A**) Representative flow cytometry plots and graph showing almost complete depletion of $CD11b^{+}Ly6G^{+}$ neutrophils in blood 48 hours post intraperitoneal injection with 500 µg anti-Ly6G antibody. (**B**) Quantitation of neutrophils in dorsal skin by MPO assay in uninfected and infected (*S. aureus*) mice pre-treated with neutrophil-depleting (Ly6G) or control antibody. Recruitment of neutrophils to infected skin at 4 hours post infection was minimal in anti-Ly6G-treated mice because of successful depletion.

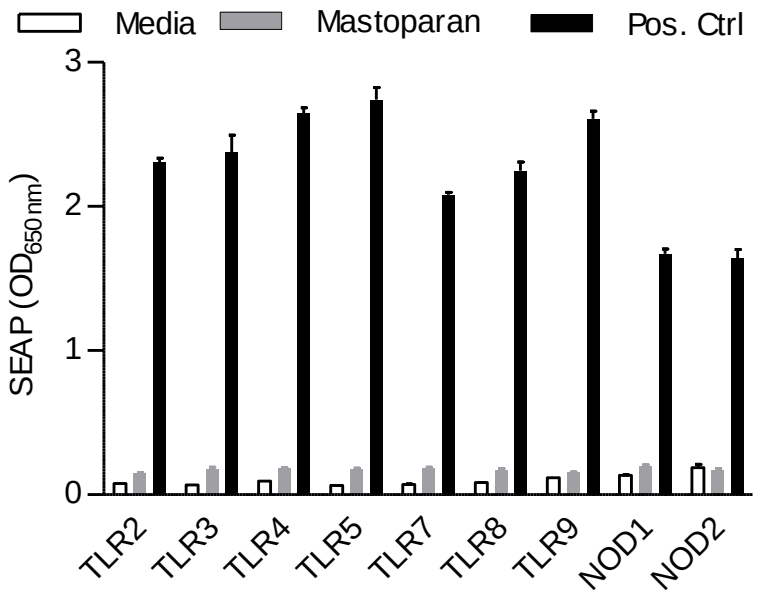

Fig. S4. Receptor-specificity of mastoparan. Quantification of activation of TLRs or NLRs by mastoparan (50 μg/ml) or positive controls specific to each receptor. SEAP, secreted embryonic alkaline phosphatase.

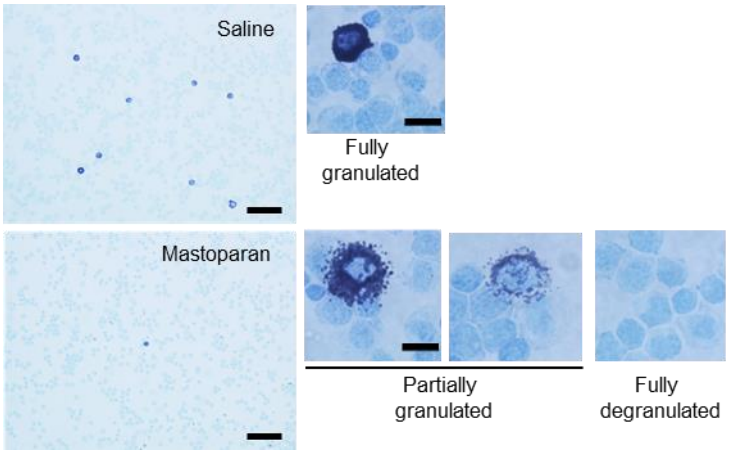

Fig. S5. Detection of granulated MCs by toluidine blue staining. Representative images of toluidine blue stained mouse peritoneal cells collected 30 min after intraperitoneal injection of mastoparan (2 mg/kg) or saline. Scale bar 50 μm. Panels on the right depict higher magnification of MCs, scale bar 10 μm. Note that in MCA-treated mice, MCs in various stages of degranulation can be detected.

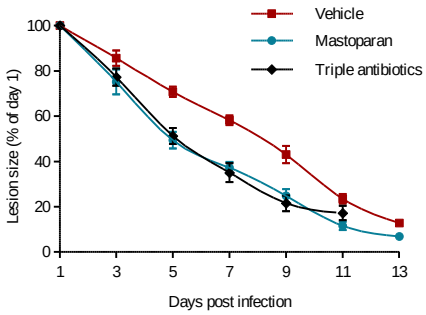

Fig. S6. Comparison of mastoparan with triple antibiotic. Lesion size of mice infected with *S. aureus* and treated with triple antibiotic (n = 18). Data of mastoparan and vehicle treatment from Fig. 3G were superimposed for comparison.

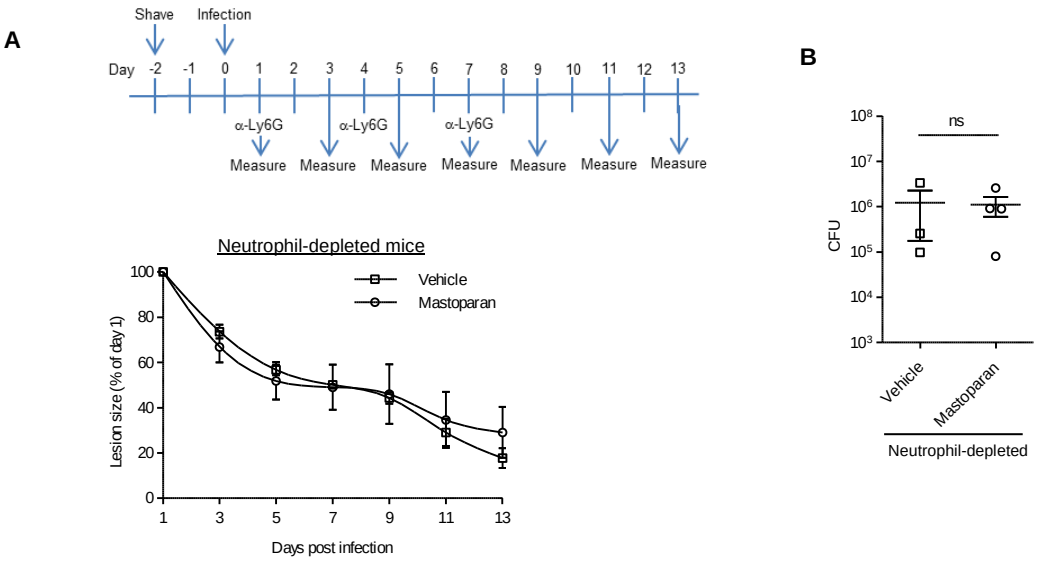

Fig. S7. Mastoparan treatment in neutrophil-depleted mice. (**A**) Schematic showing experimental plan and graph depicting mean lesion size at indicated time points post infection of neutrophil-depleted mice and treatment with vehicle or mastoparan (n = 5). (**B**) Bacterial numbers (CFUs) in the infected skin tissues day 15 post infection (n = 3-4).

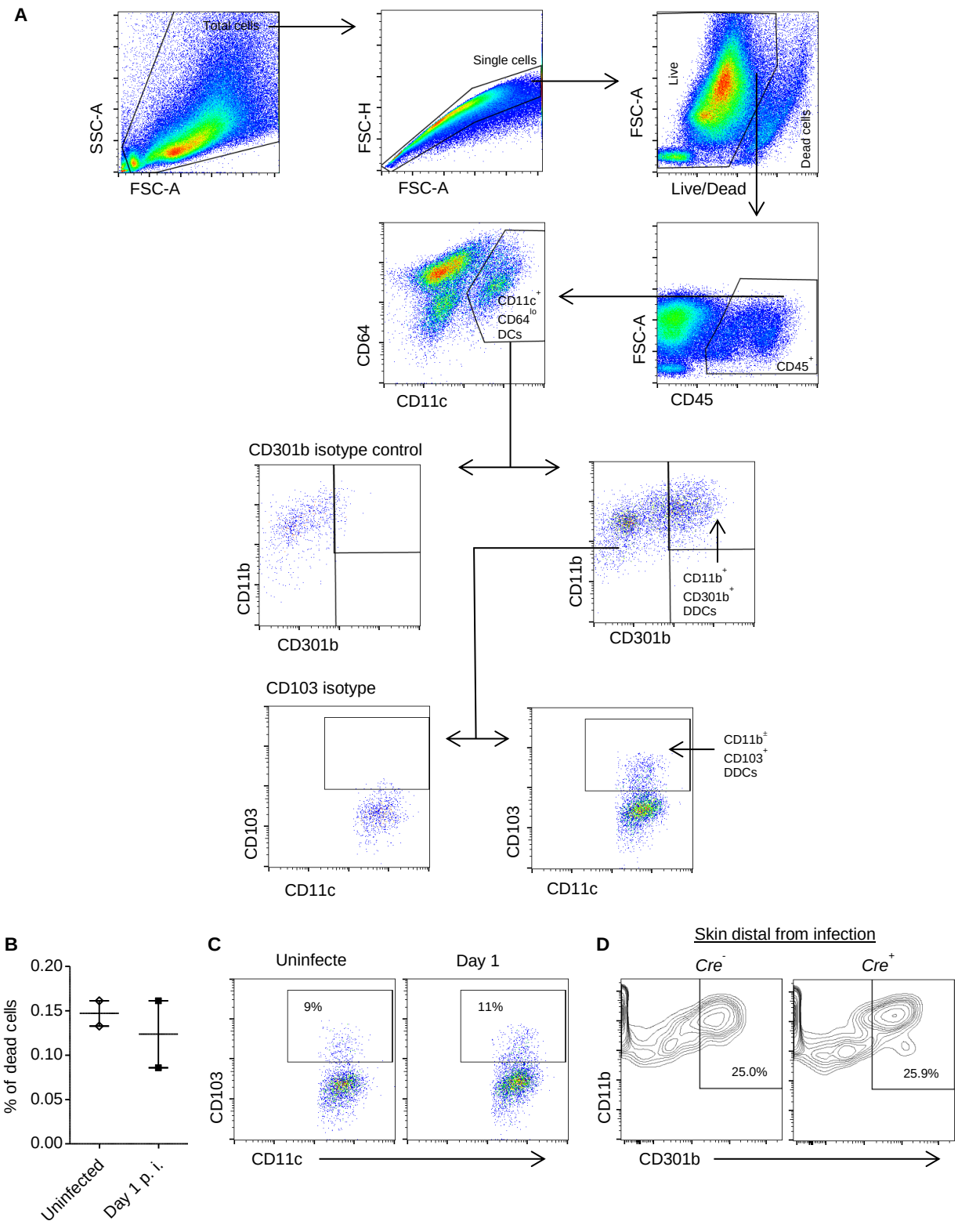
A
Total cells
SSC-A
FSC-A
Single cells
FSC-H
FSC-A
Live
Dead cells
FSC-A
Live/Dead
CD11c+ lo CD64+ DCs
CD64
CD11c
FSC-A
CD45+
CD45
CD301b isotype control
CD11b
CD301b
CD11b+ CD301b+ DDCs
CD11b
CD301b
CD103 isotype
CD11b± CD103+ DDCs
CD103
CD11c
CD103
CD11c
B
% of dead cells
0.20
0.15
0.10
0.05
0.00
Uninfected
Day 1 p. i.
C
Uninfecte
Day 1
9%
11%
CD103
CD11c
D
Skin distal from infection
Cre-
Cre+
25.0%
25.9%
CD11b
CD301b

Fig. S8. Flow cytometry plots from skin samples. (**A**) Gating strategy for flow cytometry analysis of single cell suspensions from mouse skin. (**B**) Dead CD301b$^+$ DDCs in uninfected or infected skin samples (Live/Dead$^+$CD45$^+$CD64^{lo}CD11c$^+$CD11b$^+$CD301b$^+$), shown as percent of total dead cells (n = 2). (**C**) Representative flow cytometry plots depicting CD103$^+$ DDCs in the skin with or without infection (gated from CD45$^+$CD64^{lo}CD11c$^+$CD301b$^-$ cells). (**D**) Representative flow cytometry plots depicting CD301b$^+$ DDC population (gated from CD45$^+$CD64^{lo}CD11c$^+$CD11b$^+$ cells) in skin far from infected area of various mouse groups.

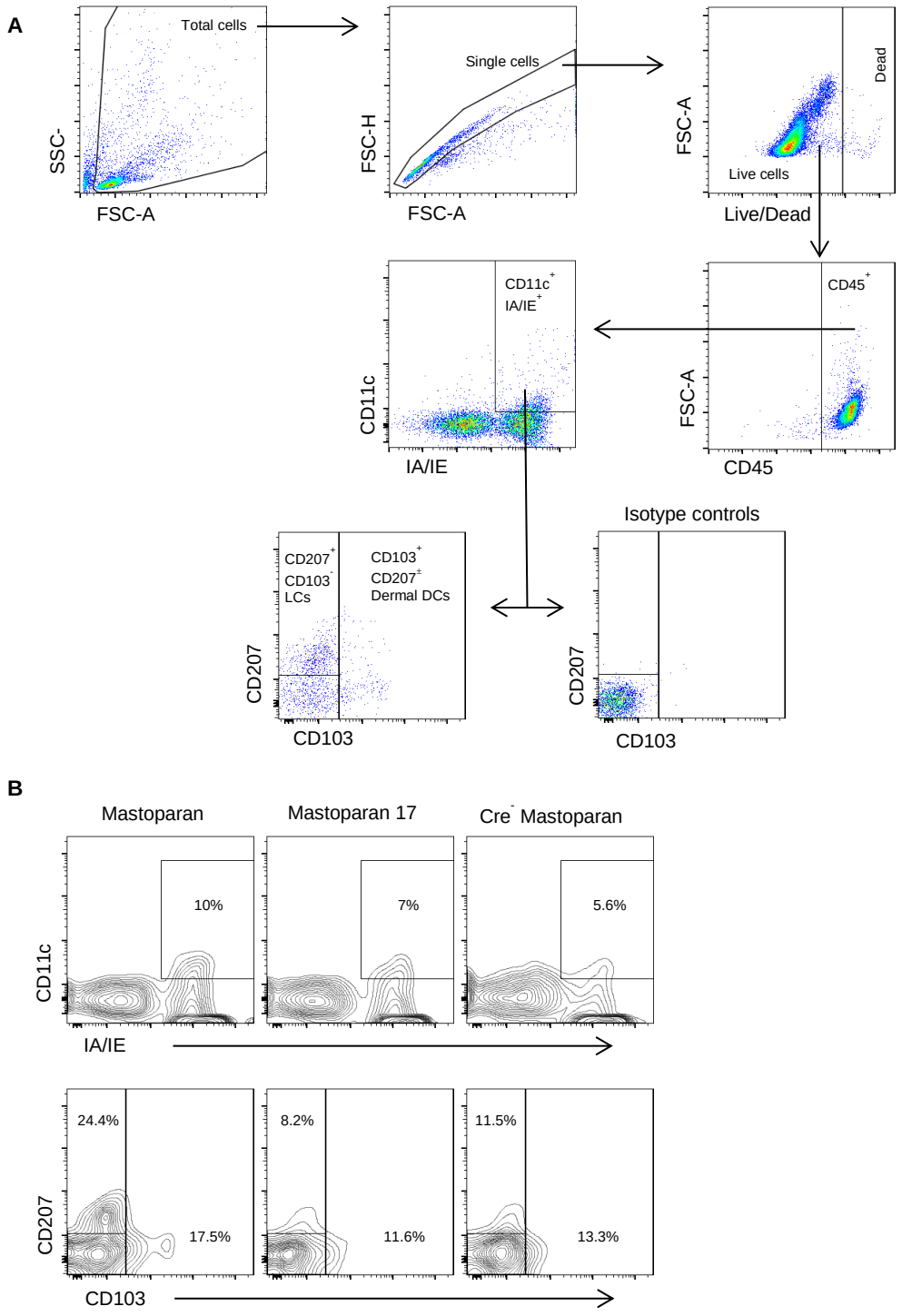

Fig. S9. Flow cytometry plots from lymph node samples. (**A**) Flow cytometry gating strategy to detect DCs in PNs. (**B**) Representative flow cytometry plots depicting IA/IE^{+}CD11c^{+} DCs, CD207^{+} LCs and CD103^{+} DDCs in PNs of various mouse groups.